Low temperature synthesis and characterisation of lecontite, $(NH_4)Na(SO_4)\cdot 2H_20$

J. THEO KLOPROGGE*
Inorganic Materials Research Program, School of Physical and Chemical Sciences, Queensland University of Technology, GPO Box 2434, Qld 4001, Australia
E-mail: t.kloprogge@qut.edu.au

MAARTEN BROEKMANS
Department of Mineral Resources, Geological Survey of Norway, N-7491, Trondheim, Norway

LOC V. DUONG
Inorganic Materials Research Program, School of Physical and Chemical Sciences, Queensland University of Technology, GPO Box 2434, Qld 4001, Australia; Analytical Electron Microscopy Facility, Queensland University of Technology, GPO Box 2434, Q 4001, Australia

WAYDE N. MARTENS, LIESEL HICKEY, RAY L. FROST1
Inorganic Materials Research Program, School of Physical and Chemical Sciences, Queensland University of Technology, GPO Box 2434, Qld 4001, Australia

Published online: 12 April 2006

Lecontite, $(NH_4)Na(SO_4).2H_2O$, was synthesised at room temperature in high purity compared to earlier work with a minor impurity of mascagnite, $(NH_4)_2SO_4$. Rietveld refinement of the XRD results confirmed the crystal structure and unit cell dimensions as published earlier. Raman and Infrared spectroscopy, in conjunction with factor group analysis, resulted in a complex pattern of overlapping sulphate, NH and OH modes. The NH modes υ_1 was observed around 2880 cm^{-1}, υ_2 around 1700 cm^{-1} overlapping with water OH-bending modes, υ_3 around 3300 cm^{-1} overlapping with water OH-stretching modes around 3023, 3185 and 3422 cm^{-1}, and υ_4 around 1432, 1447 and 1462 cm^{-1}. The sulphate group in the crystal structure displays a decrease in symmetry from T_d as evidenced by the activation of the ν_1 mode at 982 cm^{-1} and the ν_2 mode around 452 cm^{-1} in the Infrared spectrum. The υ_3 mode shows clear splitting in the infrared spectra with a strong band at 1064 cm^{-1} accompanied by two shoulders at 1107 and 1139 cm^{-1}. The Raman spectra show three weak bands at 1068, 1109 and 1135 cm^{-1} with a shoulder at 1155 cm^{-1}. Similar splitting was observed for the υ_4 mode around 611 and 632 cm^{-1} in the Infrared and Raman spectra, respectively.

1. Introduction

Lecontite, named after the American entomologist John Lawrence Leconte (1825–1883), is found in nature as a double sulphate salt $(NH_4,K)Na(SO_4).2H_20$. It belongs to the orthorhombic crystal system with spacegroup $P2_12_12_1$ and unit cell dimension $a = 8.24$, $b = 12.85$, $c = 6.24$ Å, $Z = 4$ and $V = 660.72$ Å^2. The crystal structure has been initially determined by Faust and Bloss [1] on synthetic lecontite and later by Gorazza *et al.* [2] from three-dimensional X-ray data obtained by the equi-inclination Weissenberg technique on lecontite obtained by evaporation. The lecontite structure shows chains of sodium octahedra sharing a single face with each other with a Na-Na distance of 3.15 Å. The SO_4 tetrahedron in the crystal structure is very regular. The ammonia ions coordinate to 7 oxygen atoms forming a very irregular polyhedron.

Lecontite is normally found as transparent colourless crystals with a vitreous luster and a hardness of 2 to 2.5. Its normal habit is long prismatic to massive and fine-grained. It occurs as the early product of the break-down of bat guano, e.g in the the Las Piedras Cave, near Comayagua, northwest of Tegucigalpa, Hunduras, where it was found in association with thenardite (Na_2SO_4), taylorite (discredited name = arcanite, K_2SO_4), aphthitalite

*Author to whom all correspondence should be addressed.
0022-2461
DOI: 10.1007/s10853-005-5909-5

($(K,Na)_3Na(SO_4)_2$), mascagnite ($(NH_4)_2SO_4$) and oxammite ($(NH_4)_2C_2O_4.H_2O$) [3]. Faust and Bloss synthesised lecontite through evaporation at room temperature of aqueous solutions of sodium sulphate and ammonium sulphate resulting in a mixture of lecontite and mascagnite, which were separated manually based on the differences in optical properties [1]. Gorazza *et al*. also used evaporation for the synthesis of lecontite [2].

This paper forms a continuation of earlier work in our laboratory on related sulphate minerals such as syngenite and görgeyite [4–6]. Görgeyite, $K_2Ca_5(SO_4)_6.H_2O$, is a very rare monoclinic double salt found in evaporates related to the slightly more common mineral syngenite, $K_2Ca(SO_4)_2.H_2O$. In this paper the synthesis of lecontite will be described followed by a detailed characterisation using a variety of techniques including X-ray diffraction, Scanning Electron Microscopy and Electron Microprobe analysis but with the focus on infrared and Raman spectroscopy. Up till now characterisation was basically based on X-ray diffraction of synthetic lecontite [1, 2], chemical analysis and optical microscopy (e.g. [7]). The vibrational spectroscopy has been hardly described and mainly focussed on for example the optical absorption spectra of Ni^{2+} doped lecontite [8] The paramagnetic resonance of Cr^{3+} ions in lecontite has also been studied [9], while Genin and O'Reilly have described the proton, deuterium and sodium-23 magnetic resonance spectra [10].

2. Experimental

The lecontite samples were prepared according to two preparation methods. In the first method stoichiometric amounts of 0.5 M sodium sulphate in water was added to 0.5 M ammonium sulphate in water, whereas in the second method the ammonium sulphate solution was added to the sodium sulphate solution. In both methods the resulting slurries were stirred at 25° for 20 h and then allowed to stand for 20 days. After separation the resulting solids were dried at 110°C for 1 h.

Scanning electron microscope (SEM) images were obtained on a FEI Quanta 200 Environmental Scanning Electron Microscope (FEI Company, USA) operated at an accelerating voltage of 1 kV in order to minimise the decomposition and release of ammonia from the lecontite. The powdery samples were not coated prior to use but only brought onto conducting tape, which is enough to prevent charging of the sample at such a low accelerating voltage. A gaseous secondary electron detector with a pressure limiting aperture, mounted directly above the specimen on the stage, was used for electron imaging. Elemental analysis was carried out using a thin-window EDAX energy-dispersive X-ray (EDX) detector and microanalysis system (EDAX Inc., USA).

The samples were finely ground for one minute, combined with oven dried spectroscopic grade KBr (containing approximately 1 wt.% sample) and pressed into a disc under vacuum. The transmittance spectrum of the sample was recorded in triplicate by accumulating 512 scans at 4 cm^{-1} resolution between 400 cm^{-1} and 4000 cm^{-1} using the Perkin-Elmer 1600 series Fourier transform mid-infrared spectrometer equipped with a LITA detector.

The samples were placed on a polished metal surface on the stage of an Olympus BHSM microscope, which is equipped with 10x, 20x, and 50x objectives. The microscope is part of a Renishaw 1000 Raman microscope system, which also includes a monochromator, a filter system and a CCD detector (1024 pixels). The Raman spectra were excited by a Spectra-Physics model 127 He-Ne laser producing highly polarised light at 633 nm and collected at a resolution of 2 cm^{-1} and a precision of ± 1 cm^{-1} in the range between 200 and 4000 cm^{-1}. Repeated acquisition on the crystals using the highest magnification (50x) were accumulated to improve the signal to noise ratio in the spectra. Spectra were calibrated using the 520.5 cm^{-1} line of a silicon wafer.

Spectral manipulation such as baseline adjustment, smoothing and normalisation were performed using the Spectracalc software package GRAMS (Galactic Industries Corporation, NH, USA). Band component analysis was undertaken using the Jandel 'Peakfit' software package, which enabled the type of fitting function to be selected and allows specific parameters to be fixed or varied accordingly. Band fitting was done using a Lorentz-Gauss cross-product function with the minimum number of component bands used for the fitting process. The Gauss-Lorentz ratio was maintained at values greater than 0.7 and fitting was undertaken until reproducible results were obtained with squared correlations of r^2 greater than 0.995.

The crystalline material was characterised by X-ray powder diffraction (XRD). The XRD analyses were carried out on a Philips wide-angle PW 1050/25 vertical goniometer applying CuKα radiation. The sample was measured at 50% RH in stepscan mode with steps of 0.02° 2θ and a scan speed of 1.00° per minute from 2 to 75°2θ. Rietveld analysis was performed using Retica for Windows version 1.7.7 [11]. All unit cell parameters were allowed to vary using the crystal structure published by Gorazza *et al*. [2]. Pseudo-Voigt peaks were used for the fitting, with a Lebail fitting strategy.

3. Results and discussion

Fig. 1 shows the SEM images and the corresponding EDS analysis of the synthetic lecontite. In general the material formed a conglomerate of rounded particles on which occasionally some crystal faces can be recognised. The EDS analysis is only qualitative due to the very low accelerating voltage used but does clearly show the presence of Na, N, S and O as expected for lecontite.

The crystalline nature was confirmed by XRD. Depending on which synthesis method was used small amounts of impurities were observed. In the case of the first method, where sodium sulphate was added to ammonium sulphate a small amount of mascagnite, ammonium sulphate, was observed plus a trace of thenardite, sodium sulphate, whereas in the second method only thenardite

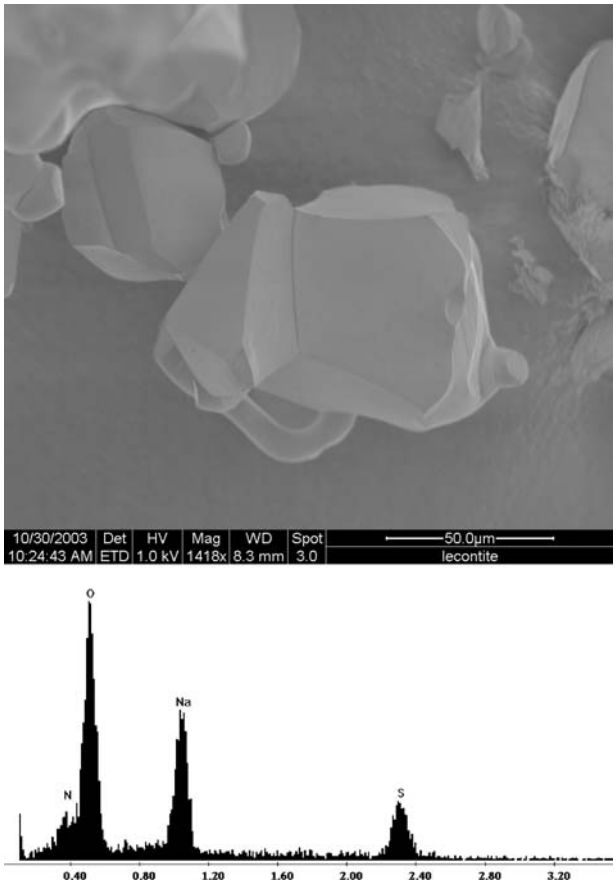

Figure 1 Low voltage SEM image and EDS analysis of synthetic lecontite.

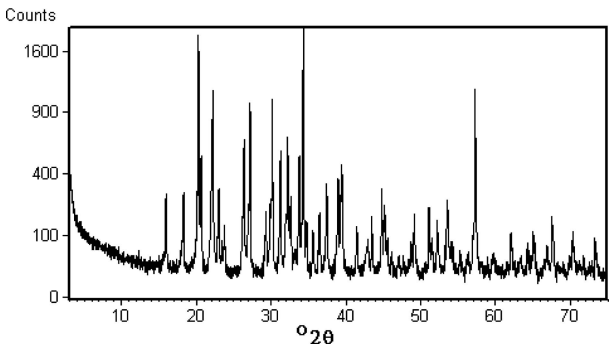

Figure 2 XRD pattern of synthetic lecontite.

was observed as a minor impurity. The majority of the thenardite reflections overlap with the lecontite reflections, but two of the strongest five reflections at 32.7 and 37.5 °2θ (d(131) 3.181 Å and d(311) 2.785 Å, respectively) can be observed as very weak reflections with 51 and 45 counts. This is in contrast to earlier work such as that of Faust and Bloss [1], where after evaporation large quantities of mascagnite were formed in addition to the lecontite. Rietveld refinement of the XRD pattern gave results within 1% of the original data reported by Gorazza *et al*. [2] (Fig. 2 and Table I).

Factor group analysis of lecontite reveals there are 201 active vibrational modes for the crystal represented by $\Gamma = 51A + 50B_1 + 50B_2 + 50B_3$. Factor group analysis of the T_d (sulphate and ammonium ions) and C_{2v} (water molecules), are shown in Tables IIa and b respectively. The ammonium ion stretching (υ_1 and υ_3) are split allowing for $4A + 4B_1 + 4B_2 + 4B_3$ modes to be present between 2800 – 3200 cm^{-1}, combined with the $4A + 4B_1 + 4B_2 + 4B_3$ applicable for the 2 independent water molecules. It is questionable in a study such as this whether all modes will be able to be accounted for due to accidental degeneracy. It is however expected that the site group splitting will be greater than the factor group splitting. This would allow for the loss of degeneracy of all vibrations.

The infrared and Raman spectra are exhibited in Fig. 3. The high wavenumber region between 2500 and 4000 cm^{-1} is characterised by a series of overlapping bands associated with the OH-stretching modes of water and the N-H stretching modes. These N-H modes are very similar to those of for example urea where N-H stretching modes are observed around 3200–3400 cm^{-1} [12–14] or in ammonium feldspars, micas [15] and clays [16, 17].

In general the υ_1 is observed around 2800- 3000 cm^{-1}, υ_2 around 1680–1750 cm^{-1}, υ_3 between 2800 and 3150 cm^{-1} and υ_4 between 1400 and 1500 cm^{-1} [18]. The ammonia stretching region of lecontite is complex due to the fact that the ammonia plus the hydroxyl stretching modes are found in the same region (Fig. 3a.). The

TABLE I Crystallographic properties of lecontite

	This study	Corazza *et al*. [2]
Crystal system	Orthorhombic	Orthorhombic
Space group	$P2_12_12_1$	$P2_12_12_1$
a (Å):	8.228	8.216
b (Å):	12.852	12.854
c (Å)	6.251	6.232
Alpha (°):	90	90
Beta (°):	90	90
Gamma (°):	90	90
Calculated density:	1.658	1.75
Volume of cell:	661.10	658.15
Z:	4	4

TABLE II A Factor group analysis of T_d molecules

	C_1	D_2
A_1		$9A$
E	$9A$	$9B_1$
$2T_2$		$9B_2$
		$9B_3$

TABLE II B Factor group analysis of C_{2v} molecules

	C_1	D_2
$2A_1$		$3A$
	$3A$	$3B_1$
B_2		$3B_2$
		$3B_3$

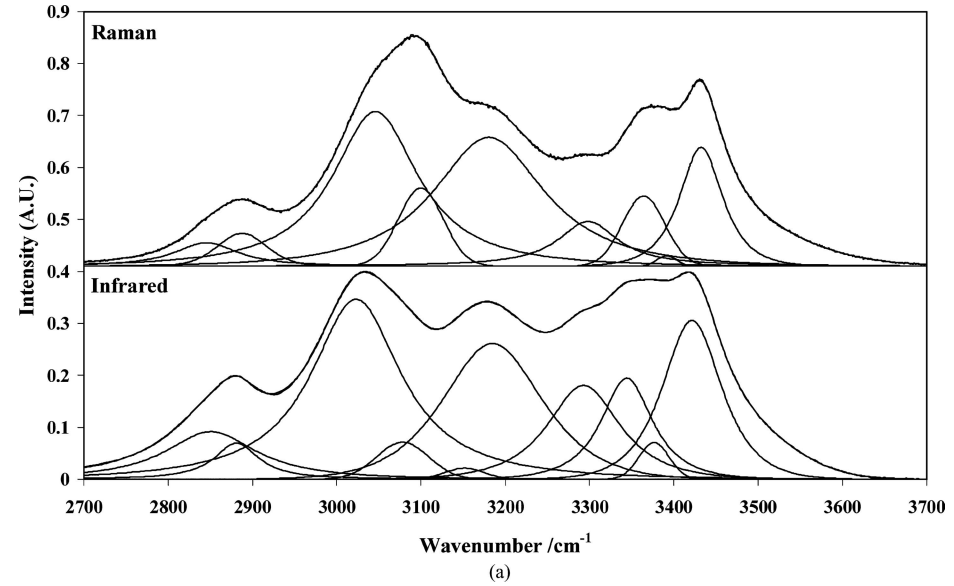

(a)

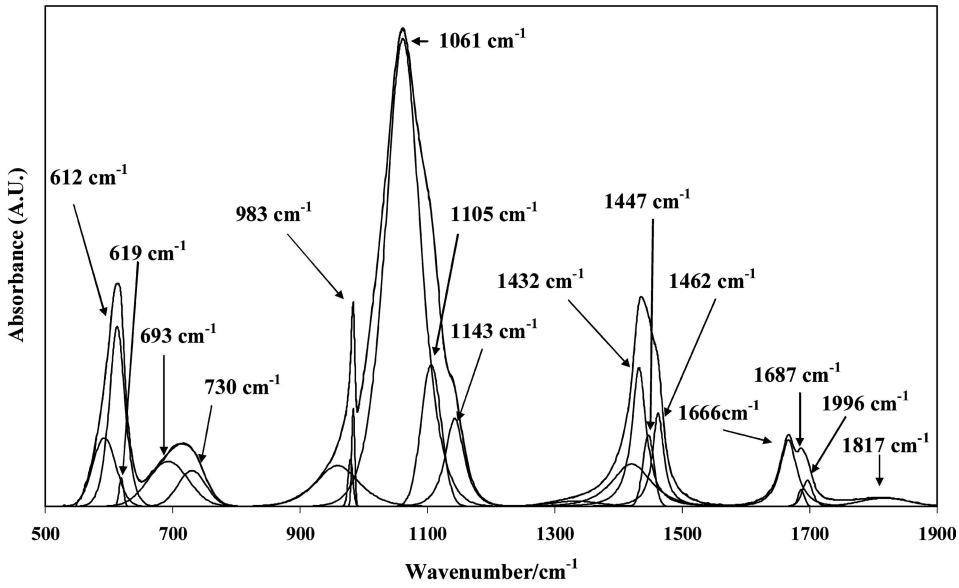

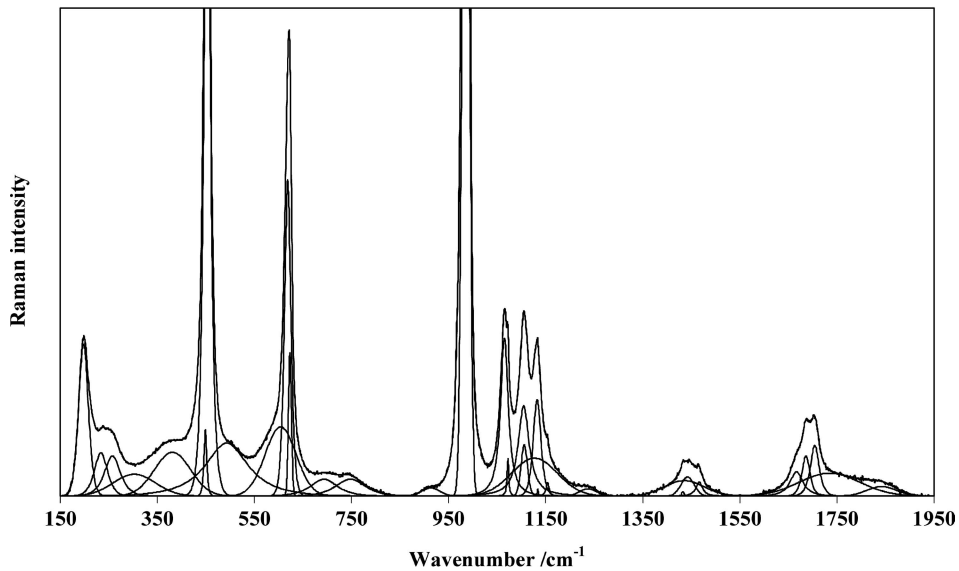

Figure 3 (a) Raman and Infrared spectra of synthetic lecontite in the region 2700 to 3700 cm^{-1}. (b) Infrared spectrum of synthetic lecontite in the 500 to 1900 cm^{-1} region. (c) Raman spectrum of synthetic lecontite in the 150 to 1950 cm^{-1} region.

water stretching vibrations are expected to behave in a similar manor to other hydrated minerals with two independent water molecules. Similarities may be drawn with the vivianite minerals where water vibrations are observed at 3050, 3220 and 3480 cm^{-1}. These vibrations would correspond to the 3023, 3185 and 3422 cm^{-1} vibrations of lecontite. Other vibrations in this region are likely to be derived from the ammonium ion. The bands at 2880 cm^{-1} are most likely the ν_1 while the vibrations found at 3293, 3344, and 3377 cm^{-1} are likely to be the ν_3 vibrations. Some vibrations in this region appear broad and ill-defined this is likely to be the fact the multiple vibrations are expected resulting in a broadening of the spectra. The ammonium ion and water vibrations also overlap in the 1600–1800 cm^{-1} region. In this region under site splitting two water bending modes and two ammonium deformation modes are expected. In this region only three bands are detected at 1666, 1687 and 1706 cm^{-1}, with broad features at ~1820 cm^{-1}. The ammonium υ_4 vibrations are expected to split in to 3 vibrations under site symmetry and are clearly seen at 1432, 1447 and 1462 cm^{-1} (Fig. 3b). Accompanying the bending mode are the OH-libration modes around 693 and 730 cm^{-1}, which are differentiated from the NH bands by their much broader bands.

Theoretically, when the sulphate retains its full symmetry (T_d) four modes of vibration will be observed: $\nu_1(A_1)$ at 983 cm^{-1}, $\nu 2(E)$ at 450 cm^{-1}, ν_3 at 1105 cm^{-1} and $\nu 4(F_2)$ at 611 cm^{-1}. The A_1 (symmetric stretching) and E (bending) modes are Raman active only, while the F_2 stretching and bending modes are both Raman and infrared active. The ν_1 mode at 982 cm^{-1} is relatively strong and very sharp in the infrared spectrum indicating a clear change in the symmetry of the sulphate group in lecontite. The corresponding Raman mode is found at 987 cm^{-1}. The ν_2 mode is observed in the infrared spectra and is also clearly visible in the Raman spectra at 452 cm^{-1}. The ν_3 is characterised by complex set of bands around 1100 cm^{-1} in both the infrared and Raman spectra due to splitting as a result of the lower symmetry of the sulphate group in lecontite. Here the bands are distinctly stronger in the infrared spectrum compared to the very weak bands in the Raman spectrum. In the infrared spectra a strong band at 1064 cm^{-1} is accompanied by two shoulders at 1107 and 1139 cm^{-1}. The Raman spectra show three weak bands at 1068, 1109 and 1135 cm^{-1} with a shoulder at 1155 cm^{-1}. The same holds for the ν_4 mode at 611 cm^{-1}, accompanied by a similar band at 623 cm^{-1} in the Raman spectra.

In conclusion, lecontite has been synthesised with much higher purity than reported in earlier work. The resulting material has been characterised by XRD and Rietveld analysis which confirmed the crystal structure determination based on hand picked grains from a synthesis mixture [1, 2]. For the first time the infrared and Raman spectra have been reported and interpreted.

Acknowledgment

The financial support and infrastructure of the Queensland University of Technology, Inorganic Materials Research Program is gratefully acknowledged.

References

1. R. J. FAUST and F. DONALD BLOSS, *Amer. Miner.* **48** (1963) 180.
2. E. CORAZZA, C. SABELLI and G. GIUSEPPETTI, *Acta. Crystallo.* **22** (1967) 683.
3. H. WINCHELL and R. J. BENOIT, *Amer. Miner.* **36** (1951) 590.
4. J. T. KLOPROGGE, R. D. SCHUILING, Z. DING, L. HICKEY, D. WHARTON and R. L. FROST, *Vibr. Spectr.* **28** (2002) 209.
5. J. T. KLOPROGGE, L. HICKEY, L. V. DUONG, W. N. MARTENS and R. L. FROST, *Amer. Mineralo.* **89** (2004) 266.
6. J. T. KLOPROGGE, Z. DING, W. N. MARTENS, R. D. SCHUILING, L. V. DUONG and R. L. FROST, *Thermo. Acta.* **417** (2004) 143.
7. C. PALACHE, H. BERMAN and C. FRONDEL, *Dana's system of mineralogy* (1951) 438.
8. S. V. J. LAKSHMAN and T. V. K. RAO, *Pramana* **20** (1983) 137.
9. L. S. EMEL'YANOVA, *Magnit. i Rezonansn. Svoistva Magnit. Materialov, Krasnoyarsk* (1980) 163.
10. D. J. GENIN and D. E. O'REILLY, *J. Chem. Phy.* **50** (1969) 2842.
11. IUCR, *IUCR Powder diffraction* **22** (1997) 21.
12. R. L. FROST and G. N. PAROZ, Clays Our Future, Proc. Int. Clay Conf., 11th (1997) 403.
13. R. L. FROST, J. KRISTOF, L. RINTOUL and J. T. KLOPROGGE, *Spectro. Acta. A.* **56** (2000) 1681.
14. J. T. KLOPROGGE and R. L. FROST, *Tijdschr. Klei, Glas Keram.* **20** (1999) 20.
15. J. H. L. VONCKEN, J. M. A. R. WEVERS, A. M. J. V. D. EERDEN, A. M. J. BOS and J. B. H. JANSEN, *Geologie en Mijnbouw* **66** (1987) 259.
16. J. T. KLOPROGGE and R. VOGELS, *Clays and Clay Minerals* **43** (1995) 135.
17. J. T. KLOPROGGE, L. HICKEY and R. L. FROST, *J. Mater. Sci. Let.* **18** (1999) 1401.
18. V. FARMER, "The Infrared Spectra of Minerals," (Mineralogical Society, England 1974).

Received 8 November 2004
and accepted 29 July 2005